Letter

Gravitational wave sources for pulsar timing arrays

Ligong Bian,[1,2,*] Shuailiang Ge,[2,3,†] Jing Shu,[3,2,4,‡] Bo Wang,[5,§] Xing-Yu Yang,[6,‖] and Junchao Zong[7,8,¶]

[1]*Department of Physics and Chongqing Key Laboratory for Strongly Coupled Physics, Chongqing University, Chongqing 401331, China*

[2]*Center for High Energy Physics, Peking University, Beijing 100871, China*

[3]*School of Physics and State Key Laboratory of Nuclear Physics and Technology, Peking University, Beijing 100871, China*

[4]*Beijing Laser Acceleration Innovation Center, Huairou, Beijing 101400, China*

[5]*International Centre for Theoretical Physics Asia-Pacific, University of Chinese Academy of Sciences, 100190 Beijing, China*

[6]*Quantum Universe Center (QUC), Korea Institute for Advanced Study, Seoul 02455, Republic of Korea*

[7]*Department of Physics, Nanjing University, Nanjing 210093, China*

[8]*CAS Key Laboratory of Theoretical Physics, Institute of Theoretical Physics, Chinese Academy of Sciences, Beijing 100190, China*

(Received 5 July 2023; accepted 9 April 2024; published 10 May 2024)

Very recently, the major pulsar timing array collaborations, including CPTA, EPTA, InPTA, NANOGrav, and PPTA, reported their results from searches for an isotropic stochastic gravitational wave background (SGWB), collectively representing positive evidence for a SGWB. In this work, we assessed the credibility of interpreting the Hellings-Downs correlated free-spectrum process of EPTA, PPTA, and NANOGrav as either the result of supermassive black hole binary mergers or various stochastic SGWB sources that originated in the early Universe, including first-order phase transitions, cosmic strings, domain walls, and large-amplitude curvature perturbations. Our results show that the current new datasets do not distinctly favor one specific SGWB source over the others based on Bayesian analysis. We also place constraints on new physics for the SGWB sources.

DOI: 10.1103/PhysRevD.109.L101301

Introduction. Pulsar timing array (PTA) experiments provide a unique window to probe the gravitational waves (GWs) at nanohertz frequencies. Very recently, NANOGrav released their new 15 yr dataset [1–3], CPTA released their first data [4], EPTA released the second data [5], and PPTA released their third dataset [6–8]. Compared to the previously observed common-spectrum process in the old NANOGrav 12.5 yr dataset [9] and the results from other collaborations like PPTA [10], EPTA [11], and IPTA [12], this time we not only have robust evidence for the common-spectrum process, but also have positive evidence concerning the Hellings-Downs (HD) correlation, which provides direct evidence for the gravitational wave quadrupolar signal.

The previously observed stochastic common-spectrum process has aroused enormous interests in the communities of astrophysics, cosmology, and particle physics. Then, numerous interpretations have been proposed in the literature with several possible sources, including supermassive black hole binaries (SMBHBs) [13–15], and cosmological sources such as cosmic strings [16–19], first-order phase transition (FOPT) [20–23], domain walls [24,25], scalar-induced GW [26–28], and so on. Wherein, the cosmic strings are generally predicted in grant unification theories [29], low-scale FOPT is well-motivated by dark matter models [30], domain walls are highly connected with axion physics [31–34], and the scalar induced GW coming from curvature perturbation that are related with formation of primordial black holes (PBHs) which may serve as part of dark matter [35–37].

In this paper, we incorporate the new PTA datasets from the three collaborations—PPTA, EPTA,[1] and NANOGrav—and employ the Bayesian analysis method

*lgbycl@cqu.edu.cn
†sge@pku.edu.cn
‡jshu@pku.edu.cn
§wangbo21a@mails.ucas.ac.cn
‖xingyuyang@kias.re.kr
¶jczong@smail.nju.edu.cn

[1]Specifically, while the common signal in EPTA DR2full exhibits mild tension compared to DR2new, they are considered consistent. Both posteriors overlap within the same $A-\gamma$ parameter region, corresponding to the fixed HD correlation power of 13/3 from SMBHBs [5]. Consequently, we utilize the more representative DR2full dataset, which already includes DR2new data.

to contrast interpretations between different SGWB models mentioned above and fit each model separately. We find that although all SGWB sources considered here could potentially explain the observations, no strong evidence clearly supports one source over the others. Considering the evidence for SGWB in the common-spectrum process is weak in the dataset of PPTA, we conservatively assume that the common-spectrum process comes from SGWB. We then place rigorous constraints on the SMBHBs, FOPT, domain walls, cosmic strings, and the scalar-induced GW with the PTA datasets. In turn, these constraints restrict relevant new physics, such as QCD scale dark matter, discrete symmetry breaking patterns, the spontaneous symmetry breaking scale of the $U(1)$ symmetry, and the PBH dark matter.

SGWB models. We discuss five main mechanisms that can generate SGWB at nano-Hertz frequencies, which are 1) SMBHBs, 2) FOPT, 3) cosmic strings, 4) domain walls, and 5) large amplitude curvature perturbations. We refer the readers to Ref. [24] and references therein for a summary of these models. For convenience, we have also summarized the GW spectra of the latter four models with corresponding references in the Appendix.

Centers of most galaxies likely host supermassive black holes, forming binary systems during galaxy mergers [38,39]. These systems emit gravitational radiation, creating a gravitational wave background (GWB) detectable in the PTA band. The GWB's properties depend on the SMBHBs' characteristics and evolution. For binaries purely evolving through GW emission, the power spectral density follows a power law with a spectral index of $-13/3$ [40], influenced by interactions with the local galactic environment [41].

FOPTs happening in the early Universe arise in many models beyond the Standard Model of particle physics. For example, they are usually associated with explaining the baryon asymmetry (see e.g., Ref. [42]). An FOPT can generate gravitational waves in multiple ways, including collisions of vacuum bubbles, relevant shocks in the plasma, sound waves in the plasma after bubble collisions, and the magnetohydrodynamic turbulence in the plasma after bubble collisions [43]. Here, following Ref. [24], we consider the scenario that sound-wave contribution dominates. The GW spectrum is mainly determined by the latent heat α_{PT}, the inverse time duration of FOPT β which is usually rescaled by the Hubble parameter H_n at the bubble nucleation temperature T_n (which is approximately T_*, the temperature when the GW are produced) and the velocity of expanding bubble wall in the plasma background v_b [43].

A cosmic string is a one-dimensional topological defect associated with a symmetry breaking of $U(1)$ symmetry, which is also predicted in many models beyond the Standard Model. Infinite strings will intersect and generate string loops [44]. The string loops can oscillate and vibrate to emit gravitational waves [45]. The strings can also develop the structure of kinks and cusps that can generate gravitational waves [46,47]. GWs emitted from cosmic strings mainly depend on the parameters $G\mu$ and α_{CS}. G is the Newton gravitational constant and μ is the string tension (energy per unit length). α_{CS} is the loop-size parameter representing the ratio of the loop size to the Hubble length (or more naturally, the correlation length [48,49]). Note we are discussing gauge strings associated with a gauge symmetry breaking, the energy of which is mainly lost in GWs, while the global strings associated with a global symmetry breaking lose energy mainly in the form of Goldstone bosons [50].

A domain wall is another kind of topological defect, which is two-dimensional. It is formed when discrete degenerate vacua are present after a symmetry breaking, which also naturally arises in many beyond the Standard Model theories. The evolution of the domain wall network can generate gravitational waves; see e.g., Ref. [51]. To avoid the domain wall problem that domain walls dominate the Universe, a bias potential ΔV is usually introduced to kill the domain wall network by explicitly breaking the vacua degeneracy [32,52,53]. ΔV determines the time when the network disappears and thus marks the location of GW spectrum's peak frequency. Another key factor is the domain wall tension σ, i.e., the energy per unit wall area.

GWs can also be generated by the curvature perturbations due to the coupling at nonlinear order between scalar and tensor modes. The large amplitude curvature perturbations are related to the formation of primordial black holes (PBHs), which are attractive dark matter candidates and are also the possible sources for the merger events of black hole binaries [35–37]. Via the coupling with the tensor modes, scalar perturbations can induce GWs; see e.g., Refs. [26–28]. The power spectrum of curvature perturbations is assumed to be a power law, $P_{\mathcal{R}}(k) \propto P_{\mathcal{R}0}(k/k_*)^m$, where k is the wave number and k_* is the wave number at the frequency around 1 yr^{-1}. The corresponding GW spectrum is then $\Omega_{\mathrm{GW}}(k) \propto P^2_{\mathcal{R}}(k)$. The amplitude $P_{\mathcal{R}0}$ and the slope m are the two key parameters that determine the GW spectrum.

Model comparisons. By using the fitting results of the free spectrum with the HD correlation from the datasets of NANOGrav, PPTA, and EPTA, we can make comparisons between the following models; SMBHBs, FOPT, cosmic strings, domain walls, and scalar-induced GWs, which are labeled as M_i ($i = 1, 2, 3, 4, 5$) in sequence, respectively. We list the Bayesian prior range of the model parameters in table. S1 in the Supplemental Material [54] and the results are summarized in Eqs. (1)–(3). In addition, the corresponding interpretation of Bayes factors is shown in Table I.

EPTA and NANOGrav have a weak evidence while PPTA has a positive evidence in favor of the cosmic strings and FOPT explanations against SMBHBs. A positive

TABLE I. Bayes factors can be interpreted as follows: for comparing a candidate model M_i against another model M_j, a Bayes factor of 20 corresponds to a belief of 95% in the statement "M_i is true", which means a strong evidence in favor of M_i. The interpretation of the value of the Bayes factor into a qualitative judgement on the evidence can be found in [55].

B_{ij}	Evidence in favor of M_i against M_j
1–3	Weak
3–20	Positive
20–150	Strong
≥150	Very strong

evidence in favor of the SMBHB, cosmic strings, scalar-induced GWs, and FOPT against domain walls is shown in all the datasets of EPTA, PPTA, and NANOGrav. NANOGrav and PPTA, especially, show more inclination in favor of the FOPT explanation than the other sources, while EPTA are more sensitive to cosmic-string explanation.

Upon comparing these explanations, we find that none of the above models has a distinct advantage over others in interpreting the common-spectrum process with the HD correlation implied in the datasets of NANOGrav, PPTA, and EPTA.

$$B_{ij}^{\mathrm{NANOGrav}} = \begin{pmatrix} 1 & 0.49 & 0.55 & 5.19 & 1.34 \\ 2.03 & 1 & 1.12 & 10.55 & 2.72 \\ 1.82 & 0.90 & 1 & 9.46 & 2.44 \\ 0.19 & 0.09 & 0.11 & 1 & 0.26 \\ 0.75 & 0.37 & 0.41 & 3.88 & 1 \end{pmatrix}, \quad (1)$$

$$B_{ij}^{\mathrm{PPTA}} = \begin{pmatrix} 1 & 0.27 & 0.32 & 2.53 & 0.58 \\ 3.64 & 1 & 1.16 & 9.2 & 2.10 \\ 3.13 & 0.86 & 1 & 7.92 & 1.81 \\ 0.40 & 0.11 & 0.13 & 1 & 0.23 \\ 1.73 & 0.48 & 0.55 & 4.37 & 1 \end{pmatrix}, \quad (2)$$

$$B_{ij}^{\mathrm{EPTA}} = \begin{pmatrix} 1 & 0.67 & 0.47 & 6.87 & 1.65 \\ 1.50 & 1 & 0.70 & 10.30 & 2.47 \\ 2.15 & 1.43 & 1 & 14.75 & 3.53 \\ 0.15 & 0.10 & 0.07 & 1 & 0.24 \\ 0.61 & 0.41 & 0.28 & 4.18 & 1 \end{pmatrix}. \quad (3)$$

Model constraints. Since no preference was found in the datasets, we thus put constraints on the parameter space of each model based on the Bayesian model fitting.

In Fig. 1, we show the constraints on the log-amplitude $\log_{10} A$ of the SMBHB power-law spectrum. Analyses of PPTA, EPTA, and NANOGrav datasets yield the results $\log_{10} A \sim [-15.04, -14.42]$, $[-14.74, -14.42]$, and $[-14.76, -14.50]$ at 68% confidence level (CL), respectively.

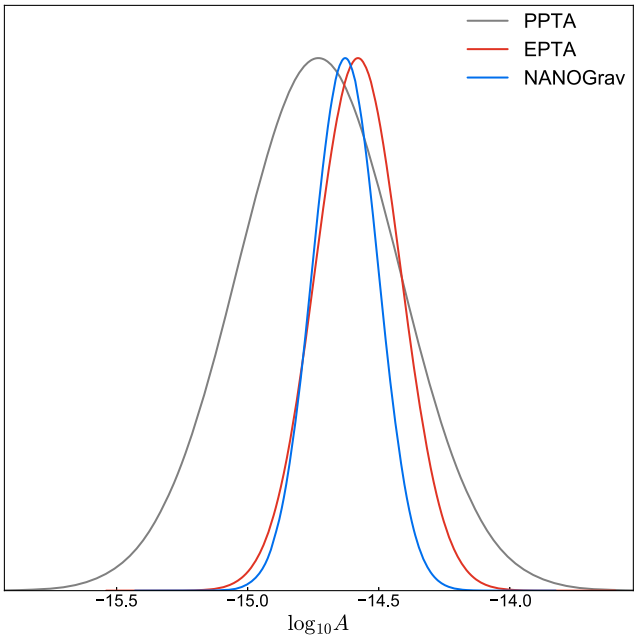

FIG. 1. Constraints on the SMBHB parameter $\log_{10} A$ from the Bayesian model fitting.

Figure 2 shows the result for the FOPT case. The data constraint based on the PPTA dataset favors a moderate latent heat $\alpha_{PT} \geq 0.548$ and a duration $\beta/H_* \sim [9, 59]$ at the phase transition temperature $T_* \sim [0.61, 1.33]$ MeV at 68% CL Likewise, EPTA dataset at the same confidence level favors a latent heat $\alpha_{PT} \geq 0.591$, accompanied by a

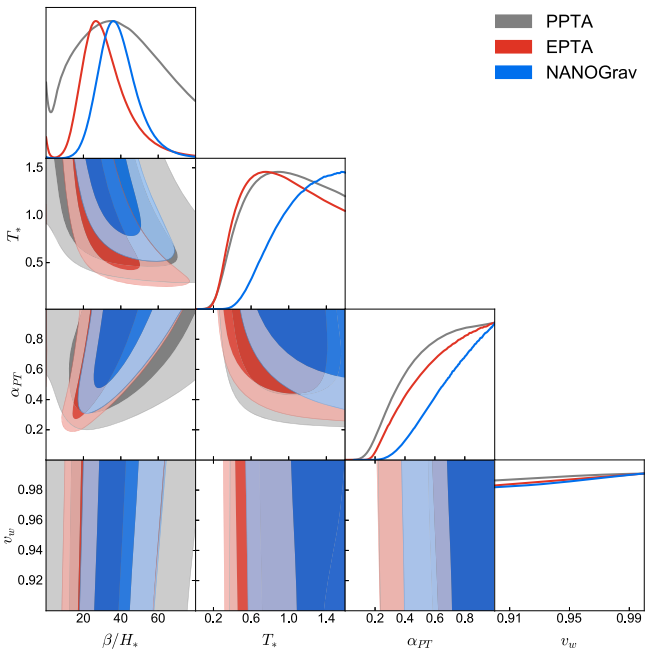

FIG. 2. The constraints on parameters of FOPT from Bayesian model fitting. Contours contain 68% and 95% of the probability.

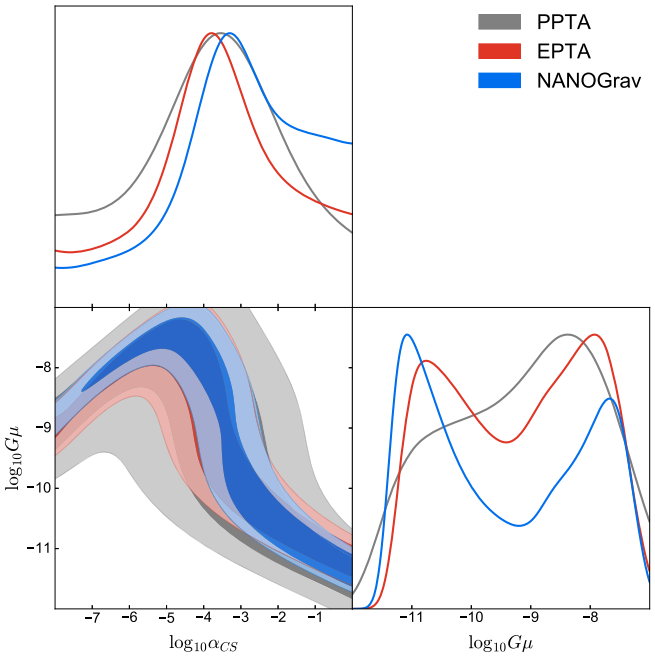

FIG. 3. The constraints on parameters of cosmic strings from the Bayesian model fitting. Contours contain 68% and 95% of the probability.

duration $\beta/H_* \sim [22, 40]$ at $T_* \sim [0.48, 1.30]$ MeV. Finally, the NANOGrav dataset at the same confidence level favors $\alpha_{PT} \geq 0.692$, $\beta/H_n \sim [29, 47]$, and $T_n \geq 1.03$ MeV. Noting that the energy injection from the phase transition would change the BBN and CMB observations [56,57], which excludes some slow and strong phase transitions around $T_* \sim 1$ MeV.

The results based on the Bayesian model fitting for the case of cosmic string network are shown in Fig. 3. The constraints yield $\log_{10} G\mu \sim [-10.2, -7.5]$, $[-10.4, -8.0]$, and $[-10.9, -8.1]$ at 68% CL under PPTA, EPTA, and NANOGrav datasets, respectively, implying a $U(1)$ symmetry-breaking scale $\eta \sim \mathcal{O}(10^{13-14})$ GeV of local strings. Meanwhile, we also obtain constraints on the loop-size parameter α_{CS} that $\log_{10}\alpha_{CS} \sim [-5.5, -1.5]$, $[-5.3, -1.5]$, and $[-4.4, -0.7]$ at 68% CL from PPTA, EPTA, and NANOGrav datasets, respectively, which are well below the typical value of $\alpha_{CS} = 0.1$ suggested by simulations [58,59].

In Fig. 4, we show the results for the domain-wall case based on the Bayesian model fitting. At 68% CL, we get tight bounds on the bias ΔV and the surface energy density σ; $\log_{10}(\sigma/\mathrm{TeV}^3) \sim [2.98, 5.12]$, $\log_{10}(\Delta V/\mathrm{MeV}^4) \leq 4.94$ under the PPTA dataset, $\log_{10}(\sigma/\mathrm{TeV}^3) \sim [2.89, 5.56]$, $\log_{10}(\Delta V/\mathrm{MeV}^4) \leq 5.26$ under the EPTA dataset, and $\log_{10}(\sigma/\mathrm{TeV}^3) \sim [5.11, 6.50]$, $\log_{10}(\Delta V/\mathrm{MeV}^4) \sim [5.50, 7.95]$ under the NANOGrav dataset. Thus, considering a Z_2 domain wall network as an example, the results imply that the symmetry breaking scale should be $\eta \lesssim 10^4$ TeV for $\sigma = 2\sqrt{2\lambda}\eta^3/3$ assuming the interaction coupling as $\lambda \sim \mathcal{O}(10^{-2})$.

In the case of scalar-induced GWs, we find $\log_{10} P_{\mathcal{R}0} \sim [-3.17, -1.67]$ and $m \sim [-1.27, 0.53]$ are allowed by the PPTA dataset, $\log_{10} P_{\mathcal{R}0} \geq -2.32$ and $m \sim [-0.12, 0.68]$

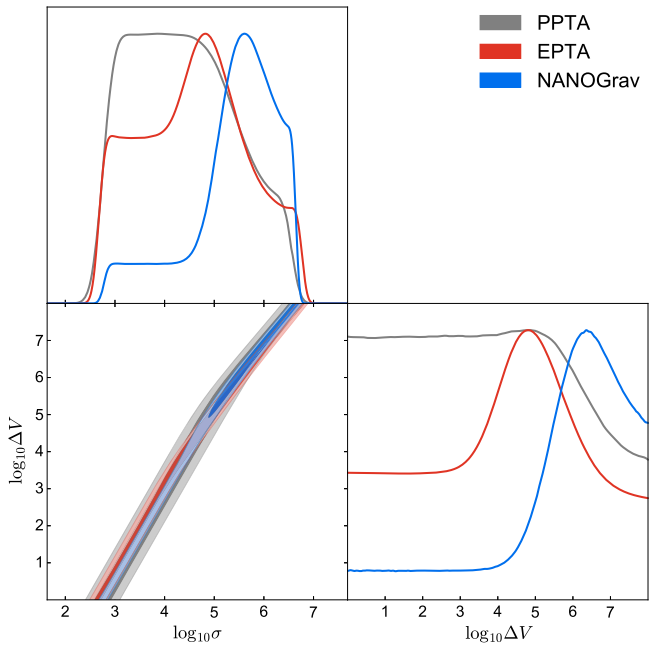

FIG. 4. The constraints on parameters of domain wall from Bayesian model fitting. Contours contain 68% and 95% of the probability.

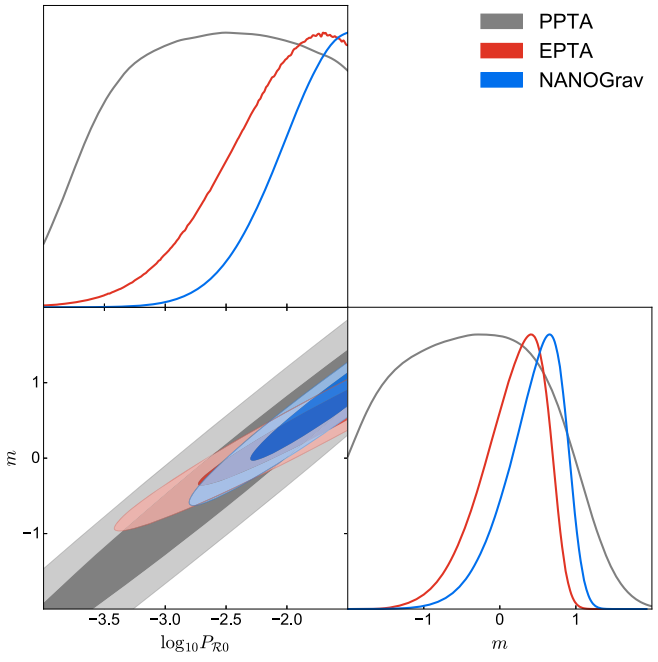

FIG. 5. The constraints on parameters of power spectrum of curvature perturbations from the Bayesian model fitting. Contours contain 68% and 95% of the probability.

are allowed by the EPTA dataset, $\log_{10} P_{\mathcal{R}0} \geq -2.03$ and $m \sim [0.19, 0.91]$ are allowed by the NANOGrav dataset at 68% CL, as shown in Fig. 5. The slope m has a negative best-fit value from the PPTA dataset, which is consistent with the result from the old 12.5 yr NANOGrav dataset. However, positive best-fit values of m are obtained from the new datasets of EPTA and NANOGrav. None of these results shows a k^3 slope which was suggested as a universal infrared behavior of GW spectrum [60]. The best-fit value of amplitude $P_{\mathcal{R}0}$ from PPTA is similar to that from the old 12.5 yr NANOGrav dataset. In comparison, the new datasets of NANOGrav and EPTA give a larger best-fit value. The larger best-fit amplitude from new datasets implies a larger corresponding PBH abundance which can be even larger if the non-Gaussianity of curvature perturbations is considered [61–63].

Conclusion and discussion. We consider different SGWB sources as the possible interpretations of the strong stochastic common-spectrum process with HD correlation observed by the NANOGrav, PPTA and EPTA collaborations. A Bayesian model comparison is carried out by fitting with the first five low-frequency bins of their HD free-spectrum data. Our results show that the current datasets from the three collaborations are unable to distinguish one SGWB model as obviously superior to the others. We also place constraints on the parameter spaces of SMBHBs, FOPT, cosmic strings, domain walls, and curvature perturbations, some of which can be further used to constrain the related new physics. Our study mainly indicates that: 1) The parameter spaces of the slow phase transition are with moderate strength around 1 MeV scale, which can be further constrained by BBN and CMB observations; 2) Cosmic strings are formed after the $U(1)$ symmetry breaking scale around $\eta \sim \mathcal{O}(10^{13-14})$ GeV; 3) The discrete symmetry breaking scale should be lower than 10^4 TeV; 4) The PBHs from curvature perturbations are severely constrained. In addition, we find that compared to EPTA and PPTA, the current data from NANOGrav can place much stronger constraints on SGWB model parameters.

Since all cosmological SGWB models can reproduce the HD signal observed in the current datasets, it is necessary to obtain more data from pulsar timing array to distinguish these models from SMBHBs. Additionally, it is important to note that more accurate GW spectra based on numerical simulations and more precise theoretical predictions of GW model parameters based on particle physics (such as the symmetry breaking scale for phase transitions, cosmic strings, and domain walls) are crucial for settling on the preferred SGWB model(s) conclusively.

Acknowledgments. This work is supported by the National Key Research and Development Program of China under Grants No. 2020YFC2201501 and No. 2021YFC2203004. L. B. is supported by the National Natural Science Foundation of China (NSFC) under Grants No. 12075041, No. 12322505, and No. 12347101, the Fundamental Research Funds for the Central Universities of China under Grants No. 2021CDJQY-011 and No. 2020CDJQY-Z003. L. B. also acknowledges Chongqing Talents: Exceptional Young Talents Project No. cstc2024ycjh-bgzxm0020. S. G. is supported by NSFC under Grant No. 12247147, the International Postdoctoral Exchange Fellowship Program, and the Boya Postdoctoral Fellowship of Peking University. J. S. is supported by Peking University under startup Grant No. 7101302974 and the National Natural Science Foundation of China under Grants No. 12025507 and No. 12150015; and is supported by the Key Research Program of Frontier Science of the Chinese Academy of Sciences (CAS) under Grants No. ZDBS-LY-7003 and CAS project for Young Scientists in Basic Research No. YSBR-006. X. Y. Y. is supported in part by the KIAS Individual Grant No. QP090701.

[1] G. Agazie *et al.* (NANOGrav Collaboration), Astrophys. J. Lett. **951**, L8 (2023).
[2] A. Afzal *et al.* (NANOGrav Collaboration), Astrophys. J. Lett. **951**, L11 (2023).
[3] G. Agazie *et al.* (NANOGrav Collaboration), Astrophys. J. Lett. **951**, L9 (2023).
[4] H. Xu *et al.*, Res. Astron. Astrophys. **23**, 075024 (2023).
[5] J. Antoniadis *et al.*, Astron. Astrophys. **678**, A50 (2023).
[6] D. J. Reardon *et al.*, Astrophys. J. Lett. **951**, L6 (2023).
[7] D. J. Reardon *et al.*, Astrophys. J. Lett. **951**, L7 (2023).
[8] A. Zic *et al.*, Pub. Astron. Soc. Aust. **40**, e049 (2023).
[9] Z. Arzoumanian *et al.* (NANOGrav Collaboration), Astrophys. J. Lett. **905**, L34 (2020).
[10] B. Goncharov *et al.*, Astrophys. J. Lett. **917**, L19 (2021).
[11] S. Chen *et al.*, Mon. Not. R. Astron. Soc. **508**, 4970 (2021).
[12] J. Antoniadis *et al.*, Mon. Not. R. Astron. Soc. **510**, 4873 (2022).
[13] V. Vaskonen and H. Veermäe, Phys. Rev. Lett. **126**, 051303 (2021).
[14] V. De Luca, G. Franciolini, and A. Riotto, Phys. Rev. Lett. **126**, 041303 (2021).
[15] K. Kohri and T. Terada, Phys. Lett. B **813**, 136040 (2021).
[16] J. Ellis and M. Lewicki, Phys. Rev. Lett. **126**, 041304 (2021).
[17] S. Blasi, V. Brdar, and K. Schmitz, Phys. Rev. Lett. **126**, 041305 (2021).

[18] R. Samanta and S. Datta, J. High Energy Phys. 05 (2021) 211.
[19] L. Bian, J. Shu, B. Wang, Q. Yuan, and J. Zong, Phys. Rev. D **106**, L101301 (2022).
[20] Y. Nakai, M. Suzuki, F. Takahashi, and M. Yamada, Phys. Lett. B **816**, 136238 (2021).
[21] A. Addazi, Y.-F. Cai, Q. Gan, A. Marciano, and K. Zeng, Sci. China Phys. Mech. Astron. **64**, 290411 (2021).
[22] W. Ratzinger and P. Schwaller, SciPost Phys. **10**, 047 (2021).
[23] X. Xue *et al.*, Phys. Rev. Lett. **127**, 251303 (2021).
[24] L. Bian, R.-G. Cai, J. Liu, X.-Y. Yang, and R. Zhou, Phys. Rev. D **103**, L081301 (2021).
[25] R. Z. Ferreira, A. Notari, O. Pujolas, and F. Rompineve, J. Cosmol. Astropart. Phys. 02 (2023) 001.
[26] K. N. Ananda, C. Clarkson, and D. Wands, Phys. Rev. D **75**, 123518 (2007).
[27] D. Baumann, P. J. Steinhardt, K. Takahashi, and K. Ichiki, Phys. Rev. D **76**, 084019 (2007).
[28] K. Kohri and T. Terada, Phys. Rev. D **97**, 123532 (2018).
[29] S. F. King, S. Pascoli, J. Turner, and Y.-L. Zhou, Phys. Rev. Lett. **126**, 021802 (2021).
[30] P. Schwaller, Phys. Rev. Lett. **115**, 181101 (2015).
[31] T. Hiramatsu, M. Kawasaki, and K. Saikawa, J. Cosmol. Astropart. Phys. 08 (2011) 030.
[32] P. Sikivie, Phys. Rev. Lett. **48**, 1156 (1982).
[33] P. Sikivie, in *Axions* (Springer, New York, 2008), pp. 19–50.
[34] T. Hiramatsu, M. Kawasaki, K. Saikawa, and T. Sekiguchi, J. Cosmol. Astropart. Phys. 01 (2013) 001.
[35] M. Sasaki, T. Suyama, T. Tanaka, and S. Yokoyama, Phys. Rev. Lett. **117**, 061101 (2016); **121**, 059901(E) (2018).
[36] M. Sasaki, T. Suyama, T. Tanaka, and S. Yokoyama, Classical Quantum Gravity **35**, 063001 (2018).
[37] B. Carr, K. Kohri, Y. Sendouda, and J. Yokoyama, Rep. Prog. Phys. **84**, 116902 (2021).
[38] J. Kormendy and L. C. Ho, Annu. Rev. Astron. Astrophys. **51**, 511 (2013).
[39] K. Akiyama *et al.* (Event Horizon Telescope Collaboration), Astrophys. J. Lett. **875**, L1 (2019).
[40] E. S. Phinney, arXiv:astro-ph/0108028.
[41] M. C. Begelman, R. D. Blandford, and M. J. Rees, Nature (London) **287**, 307 (1980).
[42] D. E. Morrissey and M. J. Ramsey-Musolf, New J. Phys. **14**, 125003 (2012).
[43] C. Caprini *et al.*, J. Cosmol. Astropart. Phys. 04 (2016) 001.
[44] T. Vachaspati and A. Vilenkin, Phys. Rev. D **30**, 2036 (1984).
[45] T. Vachaspati and A. Vilenkin, Phys. Rev. D **31**, 3052 (1985).
[46] T. Damour and A. Vilenkin, Phys. Rev. Lett. **85**, 3761 (2000).
[47] T. Damour and A. Vilenkin, Phys. Rev. D **64**, 064008 (2001).
[48] L. Sousa and P. P. Avelino, Phys. Rev. D **88**, 023516 (2013).
[49] Y. Gouttenoire, G. Servant, and P. Simakachorn, J. Cosmol. Astropart. Phys. 07 (2020) 032.
[50] A. Vilenkin and T. Vachaspati, Phys. Rev. D **35**, 1138 (1987).
[51] T. Hiramatsu, M. Kawasaki, and K. Saikawa, J. Cosmol. Astropart. Phys. 02 (2014) 031.
[52] G. B. Gelmini, M. Gleiser, and E. W. Kolb, Phys. Rev. D **39**, 1558 (1989).
[53] S. E. Larsson, S. Sarkar, and P. L. White, Phys. Rev. D **55**, 5129 (1997).
[54] See Supplemental Material http://link.aps.org/supplemental/10.1103/PhysRevD.109.L101301 for the translation of the value of the Bayes factor into a qualitative judgement on the evidence.
[55] R. E. Kass and A. E. Raftery, J. Am. Stat. Assoc. **90**, 773 (1995).
[56] Y. Bai and M. Korwar, Phys. Rev. D **105**, 095015 (2022).
[57] S. Deng and L. Bian, Phys. Rev. D **108**, 063516 (2023).
[58] J. J. Blanco-Pillado, K. D. Olum, and B. Shlaer, Phys. Rev. D **89**, 023512 (2014).
[59] J. J. Blanco-Pillado and K. D. Olum, Phys. Rev. D **96**, 104046 (2017).
[60] R.-G. Cai, S. Pi, and M. Sasaki, Phys. Rev. D **102**, 083528 (2020).
[61] R.-g. Cai, S. Pi, and M. Sasaki, Phys. Rev. Lett. **122**, 201101 (2019).
[62] N. Bartolo, V. De Luca, G. Franciolini, M. Peloso, D. Racco, and A. Riotto, Phys. Rev. D **99**, 103521 (2019).
[63] R.-G. Cai, S. Pi, S.-J. Wang, and X.-Y. Yang, J. Cosmol. Astropart. Phys. 10 (2019) 059.